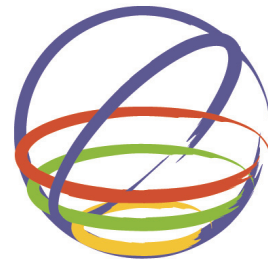


Self-Restoration Characteristics Of Granulated Blast Furnace Slag As An Earthquake Resistant Material

M. Wada, H. Matsuda, R. Ishikura & Y. Shinya

Yamaguchi University, Ube, Japan



15 WCEE
LISBOA 2012

SUMMARY:

Granulated Blast Furnace Slag (GBFS) is expected to be an useful liquefaction-resistant material because GBFS increases in shear strength with time in the ordinary natural wet condition. Authors have already clarified the physical and mechanical properties in the process of hardening by the laboratory tests and *in situ* case studies. When the structure like a backfill, in which GBFS is used and fully hardened, is collapsed by the earthquake, the shear strength is considered to recover by the self-restoration properties of GBFS. In this study, to evaluate the self-restoration characteristics of GBFS, the static and cyclic tri-axial tests were carried out for the samples, which were taken from the *in situ* embankment constructed in 2001 and were re-cured after shearing in the laboratory. In conclusion, it is clarified that GBFS has a capability of self-restoration as an earthquake resistant material.

Keywords: Shear strength, earthquake resistant material, self-restoration

1. BACK GROUND

Granulated Blast Furnace Slag (GBFS) is produced in the manufacture process of iron and the amount of production is about 190,000MN (2010) in Japan (Nippon slag association, 2011). GBFS has a latent hydraulic property and expected to become a non-liquefied material after hardening (Shinozaki, 2008; Wada, 2010; Matsuda, 2004; Matsuda, 2008). GBFS has also some advantages such as lightweight, high internal friction angle, high permeability and has already been used as a backfill material of the quay wall, landfill and lightweight embankment, etc. When GBFS is under the hardening process, especially at the early stage of hardening, it is necessary to observe the liquefaction resistance because GBFS is still a granular material and the liquefaction strength of GBFS depends on the level of hardening.

Authors have already clarified the physical and mechanical properties in the process of hardening by the laboratory tests and *in situ* case studies. After GBFS is hardened, however, when GBFS is collapsed by the earthquake motion, the shear strength is considered to recover by the self-restoration properties of GBFS. Although this is due to the latent hydraulic properties of GBFS which would be continuously remained inside the particle, its geotechnical properties including how much the shear strength would recover by the self-restoring, are not clarified yet. GBFS is a granular material, and by the reaction of hydration between particles, GBFS itself increases the shear strength. When the GBFS is collapsed by the earthquake motion after GBFS reached the solidified situation, GBFS would become a granular material in situation. Even in these situations, GBFS would have a potential to recover its shear strength. If GBFS has a self -restoration characteristic, it would be a benefit for the maintenance and/or repairing of structures after earthquake-induced disaster. In this study, self-restoration characteristics of GBFS were investigated. Firstly, the fresh GBFS was cured in the water until reaching the solidified condition, secondly solidified GBFS specimen was collapsed by cyclic loading, thirdly the collapsed specimen was cured again under some conditions and then shear strength was measured.

2. MATERIALS AND EXPERIMENTS

2.1. Test embankment and materials

In this study, two samples GBFS-A which was produced in 2004 and GBFS-B which was cured for ten years as an embankment material in the field (Matsuda, 2003; Shinozaki and Matsuda, 2003; Matsuda, 2012). Fig. 1 shows the outline of test field and embankment. The dimension of embankment is $10\text{mW} \times 20\text{mL} \times 2\text{mH}$ and the original ground of the site is composed of loose sand of 5m in thickness which is underlain by a soft alluvial clay of 6 m. The embankment was constructed by compacting to the predetermined density which is larger than 90% of the maximum density and the spreading depth was set as 0.3m/layer and 1.0m/layer.

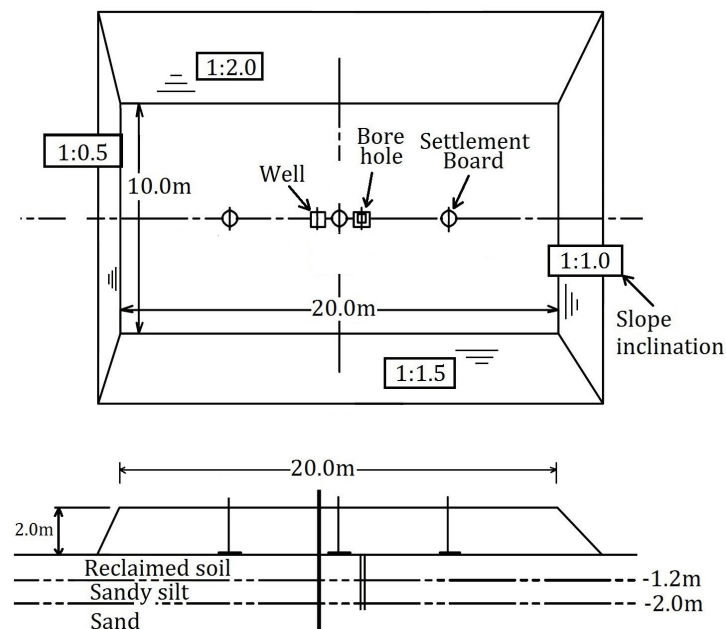


Figure 1. Test embankment constructed in 2001

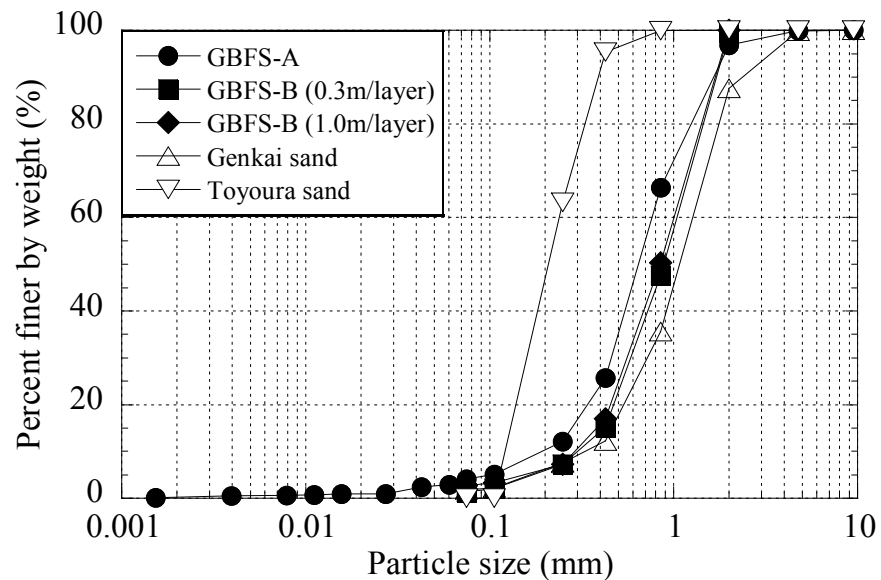
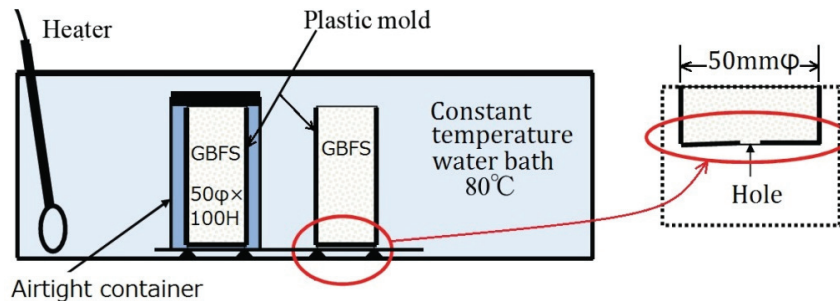
Table 1. Physical Properties Of Sample

	Specific Gravity $\rho_s(\text{g/cm}^3)$	Maximum void ratio e_{\max}	Minimum void ratio e_{\min}
GBFS-A	2.643	1.510	1.033
GBFS-B(0.3m/layer)	2.779	1.808	1.177
GBFS-B(1.0m/layer)	2.691	1.663	1.064
Genkai Sand	2.678	0.827	0.516
Toyoura Sand	2.646	0.999	0.623

Table 1 and Fig. 2 show the specific gravity, the maximum void ratio, the minimum void ratio and the particle size distribution curves for samples used in this study. In Table 1 and Fig. 2, the results for Genkai sand which is the natural marine sand and Toyoura sand which is usually used as a common sand in Japan are also shown to compare with GBFS. For specimens which are still under granular condition (GBFS-A), a saturated sample was poured into the plastic mould by controlling a relative density as $Dr=80\%$. To prepare the specimens having a different shear strength due to the hydraulic property, specimens were cured in the water with $pH \approx 8$ for predetermined duration as shown in Table

Table 2. Curing Duration

	Curing duration (days)	
	Initial curing	Second curing
GBFS-A	28	28
	56	56
	104	104
GBFS-B (0.3m/layer)	10 years in the field as an embankment	28 56

**Figure 2.** Particle size distribution curves of sample**Figure 3.** Curing in the constant temperature water bath

2 under the constant water temperature as 80 °C in order to accelerate the hardening. Fig. 3 shows the constant temperature water bath in which the specimens were cured.

2.2. Experimental method

For these specimens, two types of shear tests, i.e. the consolidated and drained tri-axial compression tests (static tri-axial test) and the un-drained cyclic tri-axial tests (cyclic tri-axial test) were performed. In all tests, specimens were saturated, where the saturated condition was confirmed by B-value to be over 0.95. When B-value is smaller than 0.95, this value was especially seen in hardened specimens,

after setting the specimen in the tri-axial test apparatus, the carbon dioxide gas was circulated through specimens by controlling the pressure inside and outside the specimen in the tri-axial cell. The static tri-axial tests were performed under the consolidation pressure of 50kPa, 100kPa and 150kPa and the cyclic tri-axial tests were carried out at 100kPa. The back pressure of 100kPa was applied to the specimen in all tests. In the static tri-axial tests, the axial load was applied to the specimen by controlling the rate of axial strain as 3%/min. In the cyclic tri-axial tests, the axial loading wave form was sinusoidal and the loading period was set as T=10s. In this study, specimens were prepared by curing in the constant temperature water bath as mentioned above.

3. SELF RESTORATION OF GBFS

3.1 Effect of cyclic shear on the particle crushing

Fig. 4 shows the particle size distribution curves on GBFS for two different situations, i.e. GBFS-A is in a fresh situation without the curing and the shearing, and the other one is once cured and collapsed by cyclic shear. It is seen that the particle size becomes a little bit finer by shearing in spite that GBFS-A is once cured and the solidified. The particle of GBFS-B is greater than that of GBFS-A.

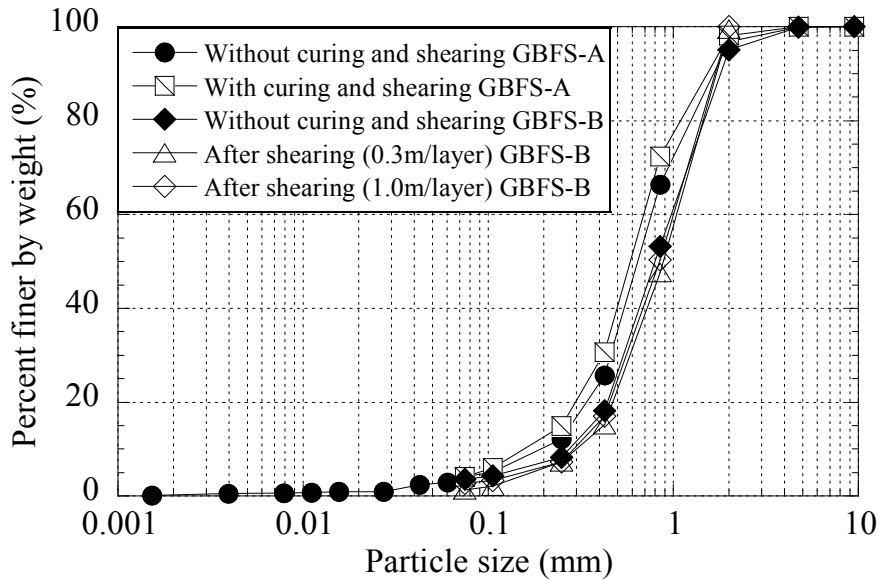


Figure 4. Grain size distribution curve of samples

3.2 Change of pH in pore water

Figs. 5(a) and 5(b) show the changes of pH due to the elution of Ca^{2+} into the pore water on GBFS-A and GBFS-B, respectively. It is seen that pH increases with curing duration on GBFS-A, in particular, when comparing the rate of increase of pH for the initial curing and the second curing, both results are almost the same. This means the rate of hardening is expected to be also the same.

3.3 Static tri-axial test

Figs. 6(a) and 6(b) show the changes of the stress ratio q/p' and the volumetric strain ϵ_v with the axial strain ϵ_a , for GBFS-A with the initial curing duration of 28 days and the second curing the same days, respectively. Where q is the principal stress difference and p' is the mean effective stress. When comparing the slope of q/p' and ϵ_a at the beginning of shear for each confining stress, the larger the confining stress, the smaller the slope of the curves becomes. This means that the particle crushing

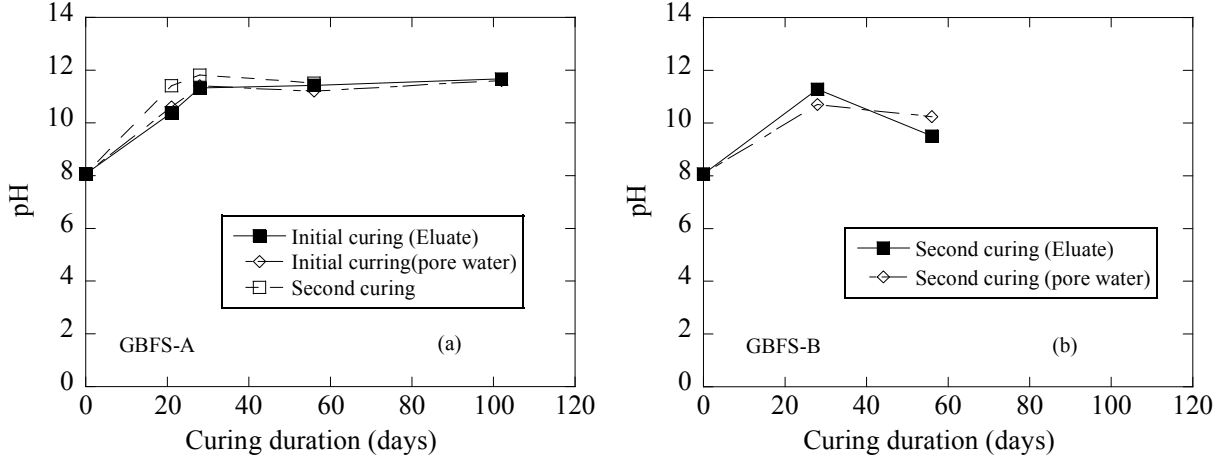
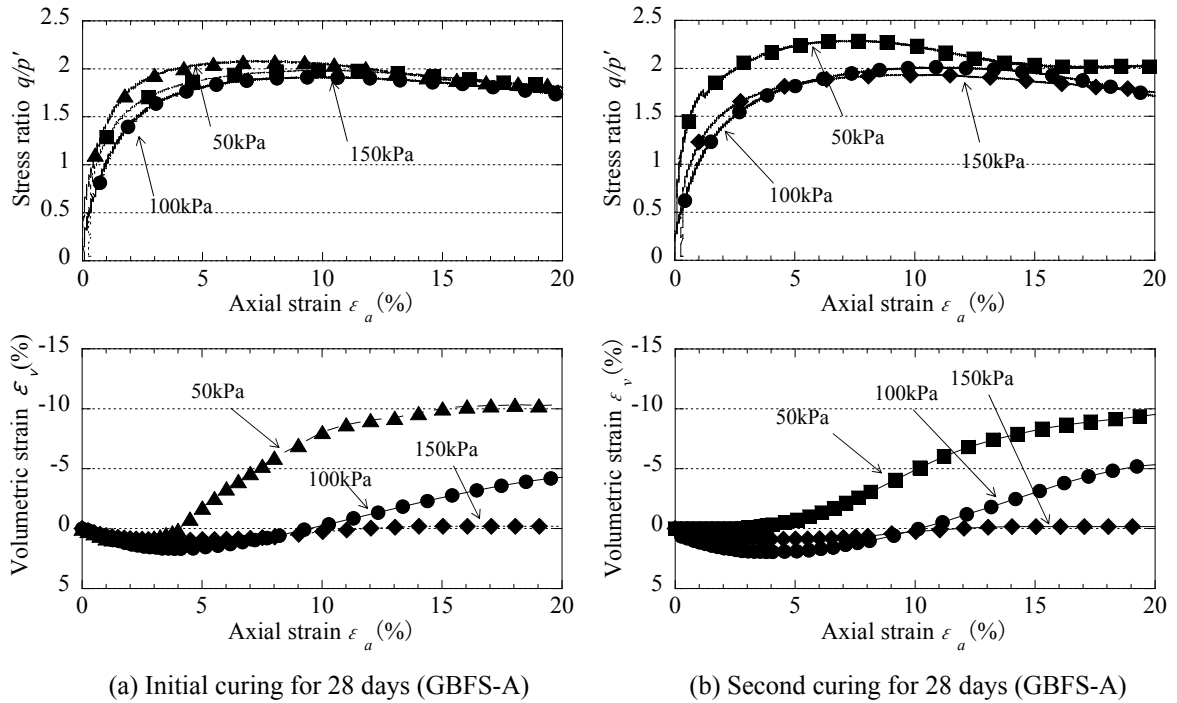


Figure 5. Relationships between pH and curing duration



(a) Initial curing for 28 days (GBFS-A)

(b) Second curing for 28 days (GBFS-A)

Figure 6. Changes of the stress ratio q/p' and the volumetric strain ε_v with the axial strain ε_a

occurs when shearing and this has been confirmed by the changes of the particle size distribution curves as shown before. As for the volumetric strain ε_v , the volume tends to move to the compression side when the effective confining pressure increases.

By the static tri-axial tests for the specimen with different curing durations, the internal friction angle φ_d and the cohesion c_d were obtained. Fig. 7 shows the relationships between φ_d and curing duration, and also between c_d and the curing duration. It is seen that the cohesion c_d increases with curing duration hence the internal friction angle is almost constant irrespective of the curing duration and keeps the value more than 35° . This tendency is the same as the results for the specimens without the curing.

In Figs. 8(a) and 8(b), the changes of stress-dilatancy characteristics of GBFS-B, which was used to construct the test embankment, are shown. Fig. 8(a) shows the results for without any curing, i.e. before construction of the embankment and Fig. 8(b) shows those for 8 years passing in the test site which is 1.5m below the top surface of the test embankment. In Fig. 8(a), the observed results are on

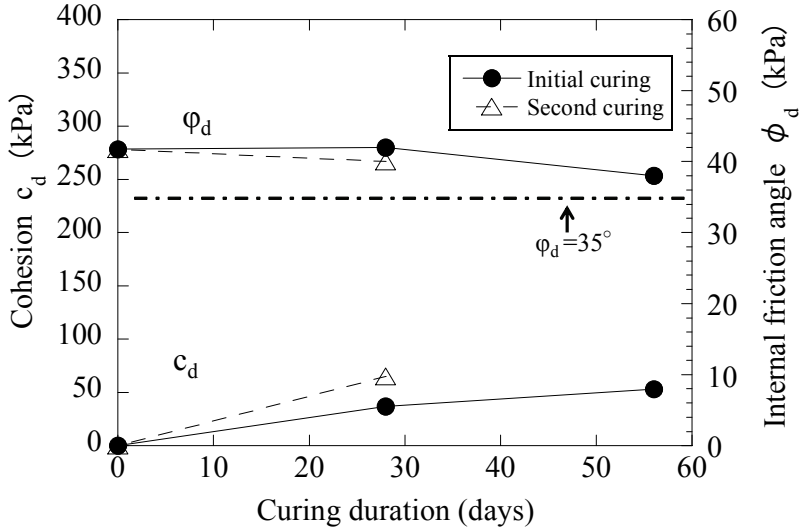


Figure 7. Changes in the angle of shear resistance ϕ_d and cohesion c_d with the curing duration

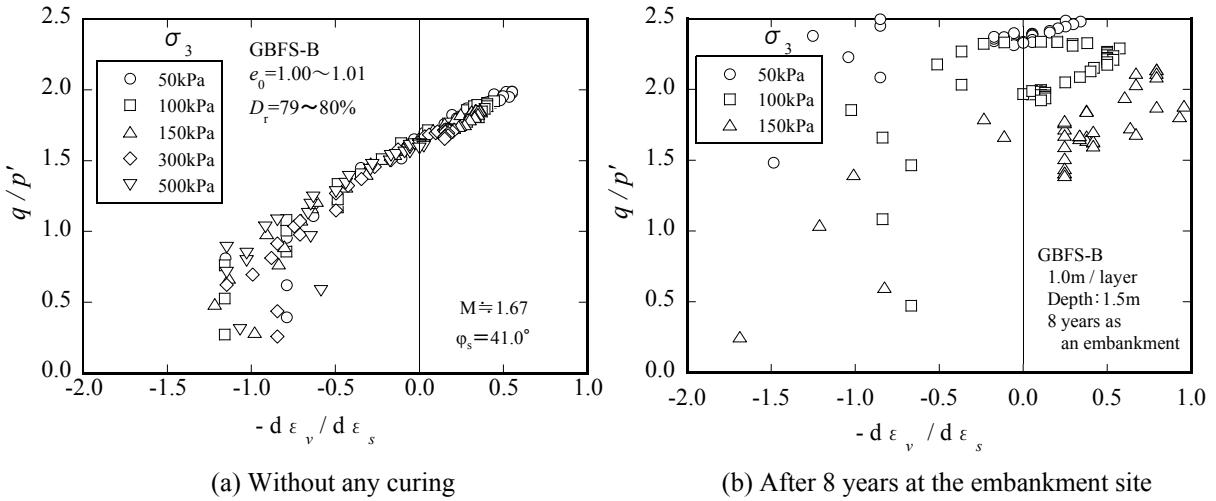


Figure 8. Effect of curing on the stress-dilatancy characteristic of GBFS-B

the same line irrespective of the confining stress and show similar characteristics to the Cam-Clay model. When GBFS passed for 8 years in the test embankment, the shear strength increases due to the increase in cohesion as shown above and the stress-dilatancy characteristics are affected by the confining stress.

3.4 Effects of secondary curing on the liquefaction resistance

The wave forms recorded for the excess pore water pressure, cyclic shear stress and axial strain are shown in Figs. 9(a), 9(b), 9(c) and 9(d) for the specimens which cured in the water for 0 days (Fig. 9(a)), 28 days (Fig. 9(b)), 56 days (Fig. 9(c)) and 102 days (Fig. 9(d)), respectively. In the case that the GBFS is in the granular situation (Fig. 9(a)), when the double amplitude axial strain DA reached 5%, it is confirmed that the excess pore water pressure increased up to the confining stress (100kPa). Therefore, in this study, the collapse was defined as the double shear strain amplitude reached 5%.

When a specimen is cured in the water for 28 days, the excess pore water pressure also increases up to the confining stress and the collapse occurs as shown in Fig. 9(b). Then the axial strain has a tendency to increase to the tension side. This means that the resistance for liquefaction of GBFS increases with the curing duration in the water. In this case, after release the confining stress, the specimen is easy to

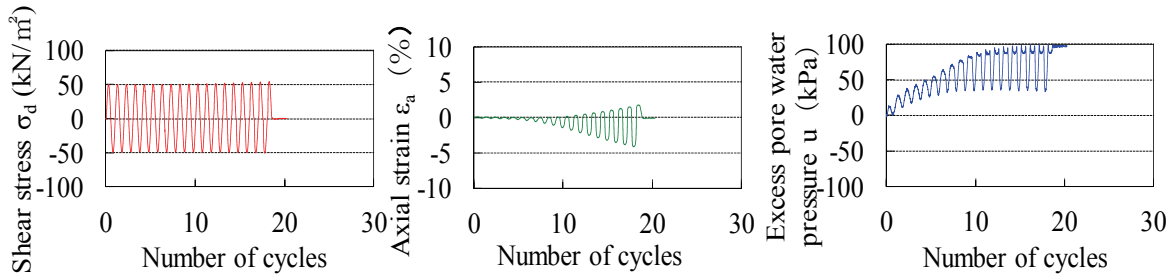


Figure 9 (a). GBFS-A Curing duration is 0 day ($\sigma_d/2\sigma_c=0.264$)

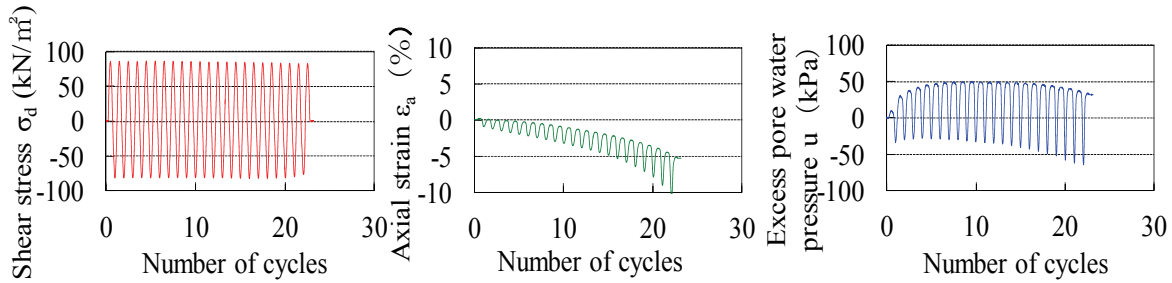


Figure 9 (b). GBFS-A Curing duration is 28 days ($\sigma_d/2\sigma_c=0.415$)

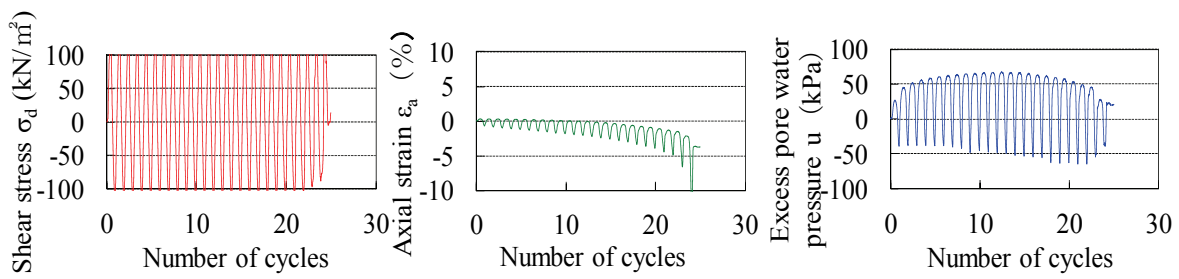


Figure 9 (c). GBFS-A Curing duration is 56 days ($\sigma_d/2\sigma_c=0.582$)

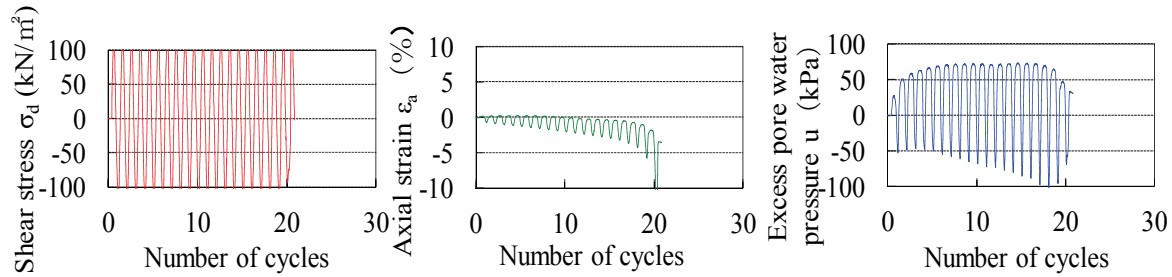


Figure 9 (d). GBFS-A Curing duration is 102 days ($\sigma_d/2\sigma_c = 0.568$)

become a granular situation by hands and this means that the bond force between each particle would disappear during cyclic shear.

When the specimen is cured for 56 days and 102 days as shown in Figs. 9(c) and 9(d), the excess pore water pressure once increased up to about 65% to 70% of the confining stress and decreases. Then the axial strain increased to a tension side and finally the specimen collapsed showing a crack line between the top surface of the specimen and the upper pedestal, or on the mid-height of the specimen. This means that the specimen is still under solidified condition and considered to be safe for the liquefaction.

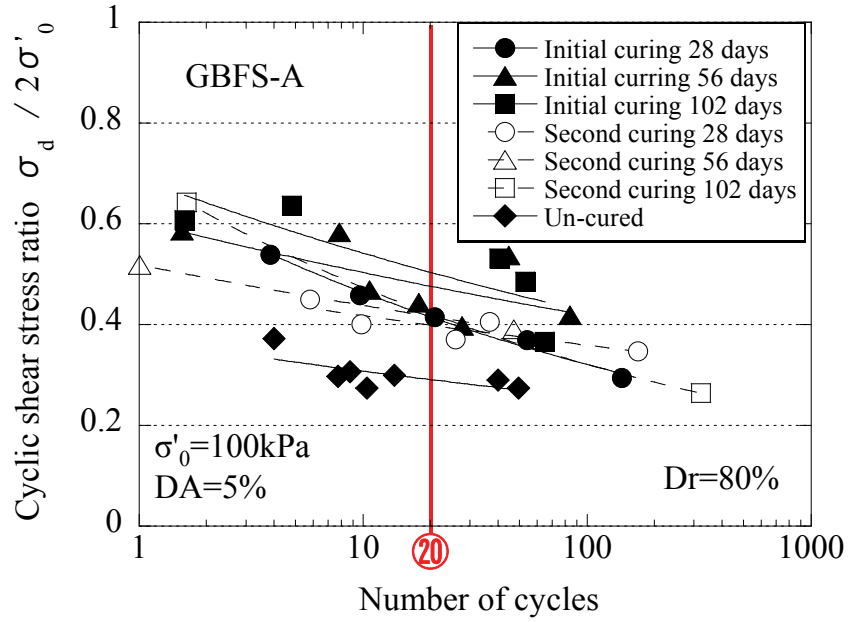


Figure 10(a). Relationships between cyclic shear stress ratio and number of cycles (GBFS-A)

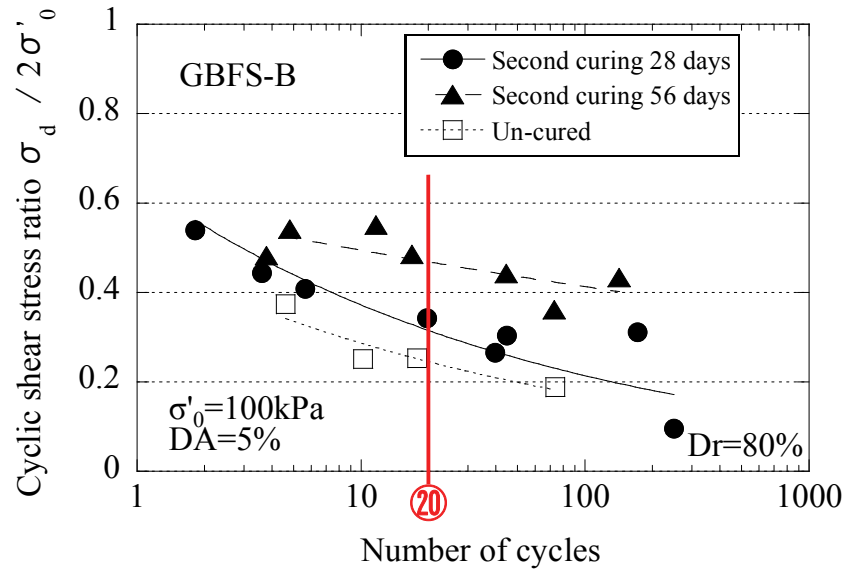


Figure 10(b). Relationships between cyclic stress ratio and number of cycles (GBFS-B)

Figs. 10(a) and 10(b) show the relations between cyclic shear stress ratio $\sigma_d/2\sigma'_0$ and the number of cycles for GBFS-A and GBFS-B. In Fig. 10(a), the longer the curing duration, the larger the cyclic shear stress ratio becomes for both the cases as initial curing and second curing, and these values are much higher than the results for the un-cured specimens. GBFS-B was taken from the embankment and once collapsed and again the second curing was applied to the specimen. In Fig. 10(b), it is seen that after two months duration of second curing, the cyclic shear stress ratio increases up to the same level as GBFS-A. This means that GBFS keeps the self-restoration characteristics for a long time, here in this study the self-restoration capability was confirmed to be kept for more than 10 years.

The relationships between the liquefaction resistance R_{20} which is defined as the cyclic shear stress ratio at the number of cycles of 20 and the curing duration are shown in Fig. 11. For all cases of curing

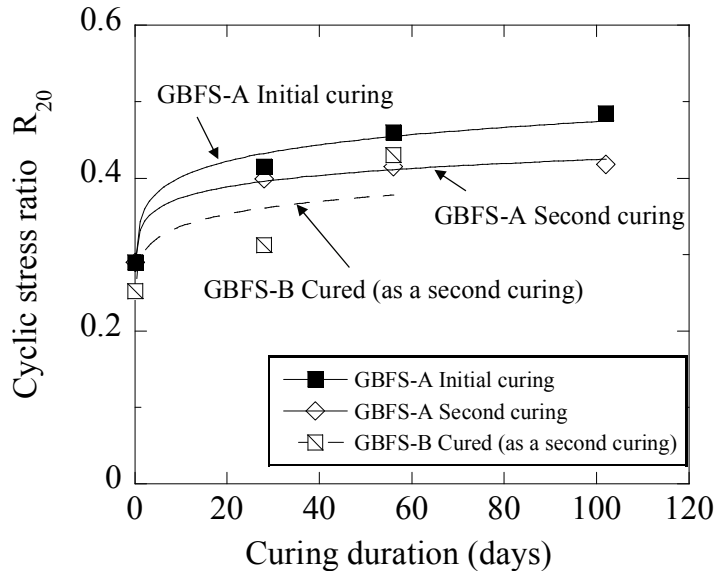


Figure 11. Relationships between cyclic stress ratio R_{20} and curing duration

patterns, R_{20} increases with the curing duration. When comparing R_{20} at the curing duration of 60 days, the highest value of R_{20} is obtained for GBFS-A with initial curing. Although the lowest one is obtained for GBFS-B with the second curing, its value is still over 0.35. This means GBFS keeps the capability of self-restoration as an earthquake resistant material.

4. CONCLUSIONS

In order to clarify the self-restoration of GBFS (Granulated Blast Furnace Slag), the static and cyclic tri-axial tests were carried out for the samples, which were taken from the *in situ* embankment constructed in 2001 and were sheared and again re-cured in the laboratory. Main conclusions obtained in this study are as follows;

- (1) The static and dynamic shear strength of GBFS, which was once solidified and then collapsed by cyclic shear, recovered by the self-restoration properties of GBFS and increased to those for the specimens initially cured in the laboratory.
- (2) Shear strength of GBFS was confirmed to increase up to the constant value, by the continuous investigation for over ten years at the *in situ* test embankment.
- (3) GBFS has a capability of self-restoration as an earthquake resistant material.

ACKNOWLEDGEMENT:

A part of this study was supported by Grant-in-Aid for Scientific Research (C), (23560993) and the experimental works were also supported by the students who graduated Yamaguchi University. The writers would like to express their gratitude to their supports.

REFERENCES

- Iron and Steel Slag, (2011). Nippon slag association.
- Shinozaki, H., Matsuda, H. and BAEK, W. (2008). Cyclic shear strength of granulated blast furnace slag in the process of hardening. *Journal of Geotechnical Engineering, Japan Society of Civil Engineers, C 64:1*, 175-180. (in Japanese)
- Wada, M., Ishikura, R. and Matsuda, H. (2010). Cyclic shear strength of granulated blast furnace slag in the non

- hardening and the process of hardening. *Ground Engineering, The Japanese Geotechnical Society*, **28:1**, 105-111. (in Japanese)
- Matsuda, H., Shinozaki, H., Okada, N., Takamiya, K. and Shinyama, K. (2004). Effects of multi-directional cyclic shear on the post-earthquake settlement of ground. *13th World Conference on Earthquake Engineering*, No.2890.
- Matsuda, H., Shinozaki, H., Ishikura, R. and Kitayama, N. (2008). Application of granulated blast furnace slag to the earthquake resistant earth structure as a geo-material. *Proceedings of the 14th World Conference on Earthquake Engineering*, 12-17.
- Matsuda, H., Ohira, N., Takamiya, K., Shinozaki, H., Kitayama, N., and Murakami, M. (2003). Application of granulated blast furnace slag to light weight embankment. *Proceedings of the international conference organized by British Geotechnical Association*, 603-611.
- Shinozaki, H. and Matsuda, H. (2003). Field tests on ground improvement using granulated blast furnace slag. *Proceedings of the international conference organized by British Geotechnical Association*, 817-824.
- Matsuda, H., Ishikura, R., Wada, M., Kitayama, N., Baek, W. and Tani, N. (2012). Aging effect on the physical and mechanical properties of granulated blast furnace slag as lightweight banking. *Japanese Geotechnical Journal*, **7**, 339-349.